CO AND CO2 HYDROGENATION OVER METAL OXIDES: A COMPARISON OF ZNO, TIO2 AND ZRO2

TEXAS UNIV. AT AUSTIN. DEPT. OF CHEMISTRY

1985

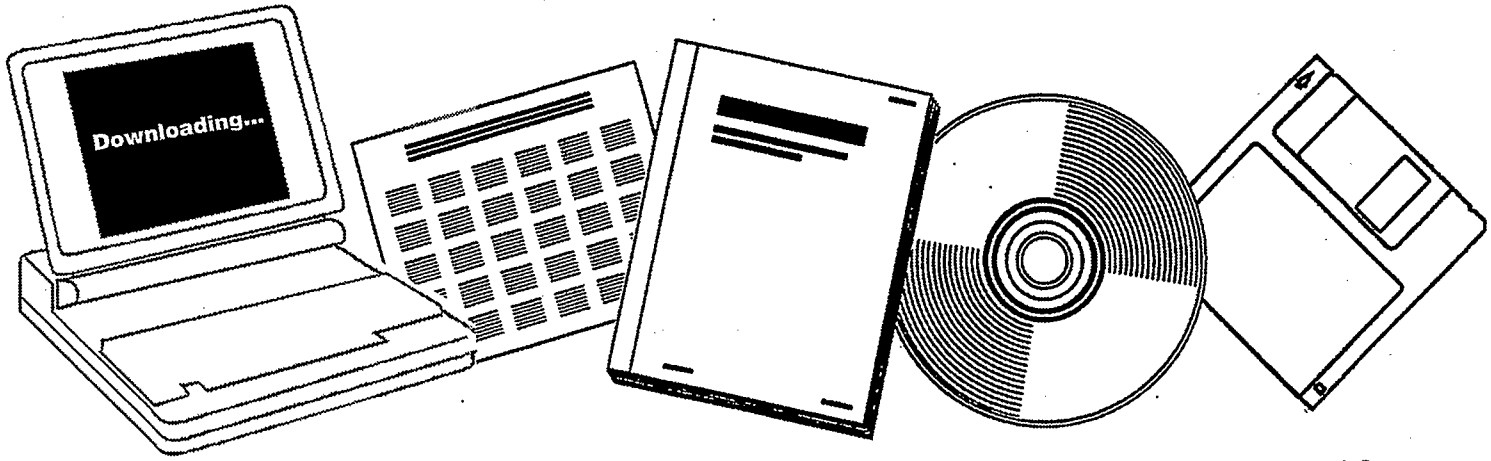

OFFICE OF NAVAL RESEARCH

Contract No. N00014-83-K-0582

Task No. NR 056-578

TECHNICAL REPORT NO. 38

CO and CO_2 Hydrogenation over Metal Oxides: A Comparison of ZnO, TiO_2 and ZrO_2

by

Ming-Yuan He, J. M. White and J. G. Ekerdt

Prepared for publication

in

The Journal of Molecular Catalysis

Department of Chemistry

The University of Texas at Austin

Austin, Texas 78712

SECURITY CLASSIFICATION OF THIS PAGE *(When Data Entered)*

REPORT DOCUMENTATION PAGE

READ INSTRUCTIONS BEFORE COMPLETING FORM

1. REPORT NUMBER	2. GOVT ACCESSION NO. / 3. RECIPIENT'S CATALOG NUMBER
4. TITLE *(and Subtitle)*: CO and CO_2 Hydrogenation over Metal Oxides: A Comparison of ZnO, TiO_2 and ZrO_2	5. TYPE OF REPORT & PERIOD COVERED: Technical Report 38, January 1 - December 31, 1985
	6. PERFORMING ORG. REPORT NUMBER
7. AUTHOR(s): Ming-Yuan He, J. M. White and J. G. Ekerdt	8. CONTRACT OR GRANT NUMBER(s): N00014-83-K-0582
9. PERFORMING ORGANIZATION NAME AND ADDRESS: J. M. White, Department of Chemistry, University of Texas, Austin, TX 78712	10. PROGRAM ELEMENT, PROJECT, TASK AREA & WORK UNIT NUMBERS: Project No. NR-056-578
11. CONTROLLING OFFICE NAME AND ADDRESS: Department of the Navy, Office of Naval Research, Arlington, VA 22217	12. REPORT DATE: June 18, 1985 13. NUMBER OF PAGES: 19
14. MONITORING AGENCY NAME & ADDRESS *(if different from Controlling Office)*	15. SECURITY CLASS. *(of this report)* 15a. DECLASSIFICATION/DOWNGRADING SCHEDULE

16. DISTRIBUTION STATEMENT *(of this Report)*

Approved for public release; distribution unlimited.

17. DISTRIBUTION STATEMENT *(of the abstract entered in Block 20, if different from Report)*

18. SUPPLEMENTARY NOTES

Reprint: J. Molecular Catalysis 30 (1985) 415-430

19. KEY WORDS *(Continue on reverse side if necessary and identify by block number)*

20. ABSTRACT *(Continue on reverse side if necessary and identify by block number)*

Infrared spectroscopy and temperature-programmed techniques are used to examine and compare the interaction of $CO/CO_2/H_2$ with three metal oxides, ZnO, TiO_2 and ZrO_2. Common surface species are formed over these oxides at 1 atm pressure, and their reactive characteristics suggest that CO hydrogenation over these oxides occurs via a formate-methoxide mechanism. Differences among the oxides were observed in that TiO_2 did not hydorgenate CO or CO_2 into methanol.

DD FORM 1 JAN 73 1473 EDITION OF 1 NOV 65 IS OBSOLETE
S/N 0102-014-6601

SECURITY CLASSIFICATION OF THIS PAGE *(When Data Entered)*

Journal of Molecular Catalysis, 30 (1985) 415 - 430

CO AND CO_2 HYDROGENATION OVER METAL OXIDES: A COMPARISON OF ZnO, TiO_2 AND ZrO_2

MING-YUAN HE,* J. M. WHITE

Department of Chemistry, University of Texas, Austin, TX 78712 (U.S.A.)

and J. G. EKERDT

Department of Chemical Engineering, University of Texas, Austin, TX 78712 (U.S.A.)

(Received April 16, 1984)

Summary

Infrared spectroscopy and temperature-programmed techniques are used to examine and compare the interaction of $CO/CO_2/H_2$ with three metal oxides, ZnO, TiO_2 and ZrO_2. Common surface species are formed over these oxides at 1 atm pressure, and their reactive characteristics suggest that CO hydrogenation over these oxides occurs via a formate–methoxide mechanism. Differences among the oxides were observed in that TiO_2 did not hydrogenate CO or CO_2 into methanol.

Introduction

The hydrogenation of CO and CO_2 gives rise to methane, methanol, oxygenated compounds and hydrocarbons. The number and distribution of products obtained imply complex mechanisms with several different paths and intermediates. When metal oxides are used as catalysts, the CO or CO_2 molecule usually does not dissociate before partial hydrogenation occurs [1, 2]. In the case of CO, possible intermediates include: HCO (formyl), H_2CO (formaldehyde), H_3CO (methoxyl), HCOH (hydroxycarbene) and H_2COH (hydroxymethyl), etc. As described by Klier [2], participation of the O-atoms of the solid oxide must also be considered and, thus, $HCOO^-$ (formate) is also a viable intermediate. Different mechanisms have been summarized [1 - 4] for methanol synthesis over metal oxides based on the reaction intermediates indicated above.

On zirconium dioxide, the surface species formed upon adsorption of CO, CO_2, CO/H_2, or CO_2/H_2 [5 - 7] and the mechanism for methanol formation [7, 8] have been investigated recently by temperature-programmed

*Present address: Research Institute of Petroleum Processing, Beijing, People's Republic of China.

0304-5102/85/$3.30

desorption and/or decomposition (TPD/TPDE), infrared spectroscopy and isotope labeling techniques. The surface species on ZrO_2 after adsorption and partial hydrogenation of CO/H_2 or CO_2/H_2 include bicarbonate, formate, oxymethylene (H_2COO^-) and methoxide. Methanol formation over ZrO_2 is thought to occur by two different mechanisms; one involves surface methoxide while the other involves a surface methyl formate-like species as the precursor. The investigation of both surface C_1 and C_2 intermediates shows that the formate is indeed a key intermediate in CO or CO_2 hydrogenation over ZrO_2.

Among metal oxides, ZnO is widely used in industry as a catalyst for methanol synthesis [2]. The adsorption and hydrogenation of CO and CO_2 on ZnO has been investigated by many researchers [9 - 15]. Since dissociative H_2 chemisorption and the formation of Zn—H bonds occur [16, 17], a reaction between Zn—H and adsorbed CO is expected and would generate a formyl intermediate. The formation of the surface formyl on ZnO upon adsorption of CO/H_2 has been confirmed by IR spectroscopy [10, 11]. The addition of hydridic hydrogen to CO also occurs in homogeneous metal complex chemistry [18]; however, the reaction is generally reversible and the equilibrium favors the reactants [19 - 21]. It has also been suggested that the formation of formyl species may be promoted by Lewis acids or strong protonic acids on the surface [19]. Using IR methods, surface formate and methoxide have also been identified on ZnO from CO/H_2, CO/H_2O and CO_2/H_2 exposure [22, 23]. Similar results have been obtained using temperature-programmed desorption studies [13, 14] and chemical trapping techniques (on ZnO/Cr_2O_3) [24]. The formate–methoxide mechanism was proposed as a major pathway and the formyl mechanism ($CO/H_2 \rightarrow$ formyl $\rightarrow$ formaldehyde $\rightarrow$ methoxide $\rightarrow$ methanol) as a minor pathway to methanol on ZnO [13]. A formaldehyde mechanism has also been suggested for CO or CO_2 hydrogenation, since formaldehyde was found among the products of methanol decomposition [25 - 27]. However, the existence of formaldehyde in the products of methanol synthesis on ZnO has never been reported. Further study of CO and CO_2 hydrogenation over ZnO is needed to unravel the complex details.

TiO_2 has not been widely studied as a catalyst for CO and CO_2 hydrogenation. Compared to ZrO_2 and ZnO, TiO_2 is much more acidic, and typically shows a dehydration rather than dehydrogenation activity. Distinctive mechanistic features based on a pathway that bypasses the formate intermediate have been reported for transition metal-based catalysts such as Rh/TiO_2 [28]. The adsorption of CO and CO_2 have been reported on TiO_2 [29] and Pt/TiO_2 [30, 31] hydrated rutile surfaces [32].

In this paper we compare three different metal oxides, ZrO_2, ZnO and TiO_2, as catalysts in CO and CO_2 hydrogenation. Our results show that the formate–methoxide mechanism is applicable to all three metal oxides. Both low- and high-temperature methanol formation paths and the formation of a methyl formate-like species were observed on ZnO, as on ZrO_2 [8]. For TiO_2, no methanol was found in the products.

Experimental

The metal oxide was placed in a 12.7 mm o.d. quartz tube fitted with a quartz frit. The tube was positioned in a furnace which was heated linearly at 1 °C s^{-1}; the catalyst temperature increased linearly between 100 and 550 °C. Gas at 1 atm flowed through the bed at a rate of 30 standard cm^3 min^{-1} (SCCM). This flow is slow enough to allow equilibrated readsorption [33, 34]. A small portion of the effluent gas was admitted to a UTI 100C quadrupole mass spectrometer (MS) through a series of two 0.07 mm orifices. A Peak Selector capable of monitoring 9 mass channels as a function of time was used to collect the data.

The oxide samples consisted of 2.0 g ZrO_2 (5.8 m^2 g^{-1} BET area (Alfa–Ventron)), 2.0 g ZnO (4.4 m^2 g^{-1} BET area (Fisher Z-52)), or 0.5 g TiO_2 (50.0 m^2 g^{-1} BET area (Degussa P-25)).

A typical procedure involved heating the oxide to 600 °C in flowing oxygen and maintaining it at 600 °C for 0.25 h followed by flushing with helium and cooling to 25 °C in flowing helium. The adsorbate gas was admitted at 25 °C, and the temperature was then increased to 600 °C and reduced to 25 °C in the flowing adsorbate gas. This adsorption procedure was followed to give ample opportunity for the different structures, which may require elevated temperatures, to form. The adsorption of HCOOH, CH_3OH and $HCOOCH_3$ was done by bubbling He (30 ml min^{-1}) through the liquid and passing the He vapor mixture over the oxide at 25 °C. The carrier gas was changed to hydrogen or helium, and the temperature was subsequently ramped at the constant rate of 1 °C s^{-1}.

The hydrogen (Matheson UHP, 99.999%) was passed through a deoxo cylinder and a bed of 4A molecular sieves to remove oxygen and water. Carbon monoxide (Matheson UHP, 99.8%) was heated to 180 °C over molecular sieves to decompose metal carbonyls. Helium had a minimum purity of 99.995% and was passed through a bed of 4A molecular sieves to remove water.

All the IR measurements were taken with the metal oxide wafer at 25 °C. Before adsorption, the wafer of metal oxide was treated in oxygen at 500 °C for 2 h followed by evacuation (10^{-3} torr) for 1 h at 500 °C.

Results

The heating rate (1 °C s^{-1}) and carrier flow (30 SCCM) were held constant for all TPD/TPDE experiments. In the case of ZrO_2, desorbed species were observed at five distinct temperature regions (Table 1) for all the experiments. For the purpose of comparing the different metal oxides used, common desorption regions for ZrO_2, ZnO and TiO_2 are also denoted in Table 1. The assignment of the decomposing species is based on indirect chemical evidence consistent with all of the IR and TPD/TPDE results [5, 8]. Additional detail is given in the Discussion section of this paper.

TABLE 1

Desorption temperature regions (°C)

Region	Decomposing species	ZrO_2	ZnO	TiO_2
I	molecular CO	40 - 60	—	40 - 50
II	carbonate and bicarbonate	120 - 420	120 - 430	90 - 370
III	methoxide	460 - 510	430 - 480	400 - 450
IV	formate	580 - 620	460 - 500	460 - 500
V	C_2 species	580 - 610	580 - 600	—

TABLE 2

TPD/TPDE into flowing H_2 of CO, CO_2, CO/H_2 and CO_2/H_2 adsorbed on ZrO_2, ZnO and TiO_2

Oxide	Dose gas	Product desorption temperature peak regions				
		I[a] (molecular CO)[b]	II (carbonate)	III (carbonate)	IV (methoxide)	V (C_2)
ZrO_2	CO	CO	CO_2	CO	$CH_4 > CO$	CH_3OH
	CO_2		$CO_2 > CO$		$CH_4 > CO$	$CH_3OH > CO_2$
	CO/H_2		CO_2			$CO_2 > CH_3OH > HCOOCH_3$
	CO_2/H_2		CO_2			$CO > CH_3OH > HCOOCH_3$
ZnO	CO		CO	$CO > CO_2$	CH_4	
	CO_2		$CO_2 > CO$	$CO > CO_2$		
	CO/H_2			$CO > CO_2$		$CH_3OH > H_2CO$
	CO_2/H_2			$CO > CO_2$		
TiO_2	CO	CO	CO_2	$CO_2 > CO$	CH_4	
	CO_2		$CO_2 > CO$	CO_2	CH_4	
	CO/H_2		CO_2	CO_2	CH_4	
	CO_2/H_2		$CO_2 > CO$	$CO_2 > CO$	CH_4	

[a]See Table 1 for identification of temperature ranges.
[b]Proposed desorbing/decomposing species.

TPD/TPDE of CO, CO_2, CO/H_2 and CO_2/H_2

The hydrogenation of preadsorbed CO, CO_2, CO/H_2 and CO_2/H_2 during the TPD/TPDE process was followed using hydrogen as the carrier gas. A summary for ZrO_2 [5, 8], ZnO and TiO_2 is given in Table 2. The TPD/TPDE products of surface species and their relative quantitation are indicated. The temperature range corresponding to the column headings are given in Table 1 and the species assignments are indicated in parentheses. The C_2 designation refers to one or more surface species which react/decompose to give one or

more of the following products at elevated temperatures: methyl formate, methanol, formaldehyde and a product with a mass signal of 45. The TPD/TPDE spectra of preadsorbed CO and CO/H_2 on ZnO and TiO_2 are shown in Figs. 1 - 4, respectively. There are two temperature regions for each experiment which are assigned to carbonate decomposition. No further dissection of these was made into monodentate, bidentate or bicarbonate species. Trace amounts of CO and CO_2 were also detected in the methoxide region when methane signals were relatively large (Fig. 3), but these are not indicated in Table 2. The TPD/TPDE of preadsorbed CO on hydrogen-treated TiO_2 (heated to 600 °C in H_2) gave a spectrum (not shown) similar to that in Fig. 3, except only trace amounts of CO and CO_2 were found at 330 - 370 °C.

TPD/TPDE of CH_3OH, HCOOH and $HCOOCH_3$

The TPD/TPDE of preadsorbed CH_3OH, HCOOH and $HCOOCH_3$ were also done in flowing hydrogen to gather data for comparison with products formed during TPD/TPDE of CO, CO_2, CO/H_2 and CO_2/H_2 (Table 2). Since surface formate is apparently easily hydrogenated to other species, as evidenced by the absence of surface formate in Table 2, the TPD/TPDE of HCOOH was also conducted using He instead of H_2 as the carrier gas. The

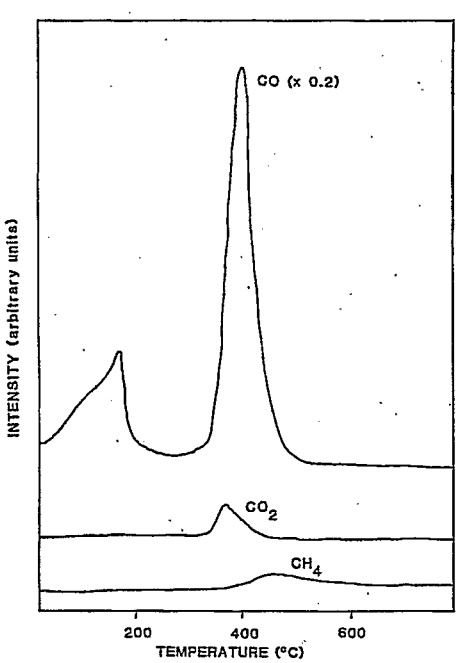

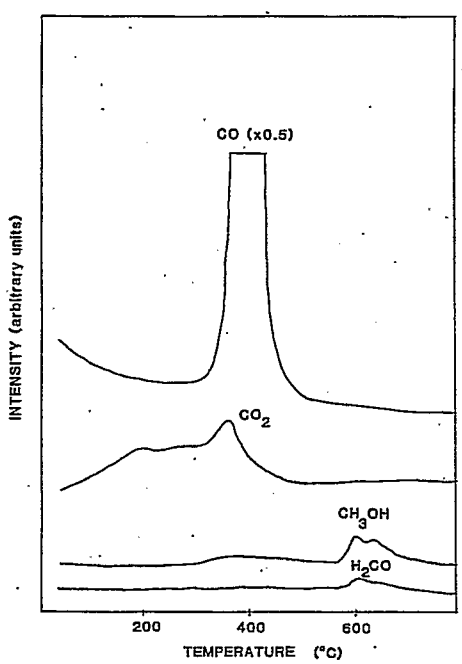

Fig. 1. TPD/TPDE from ZnO of preadsorbed CO into flowing H_2.

Fig. 2. TPD/TPDE from ZnO of preadsorbed CO/H_2 into flowing H_2.

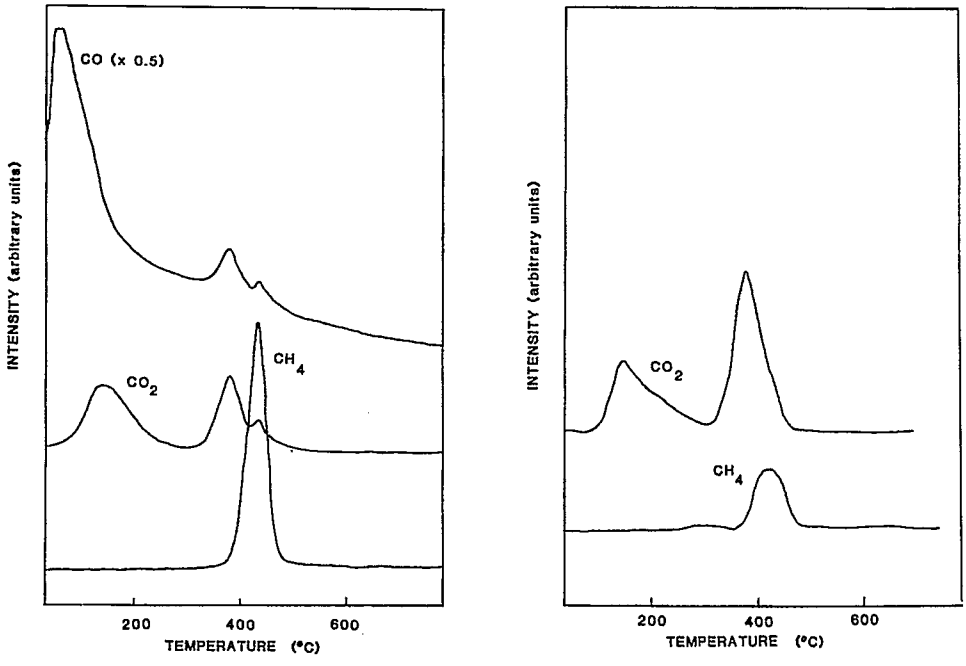

Fig. 3. TPD/TPDE from TiO_2 of preadsorbed CO into flowing H_2.

Fig. 4. TPD/TPDE from TiO_2 of preadsorbed CO/H_2 into flowing H_2.

results for ZrO_2, ZnO and TiO_2 are listed in Table 3. The details for ZrO_2 have been presented earlier [5, 8]. The TPD/TPDE spectra of preadsorbed CH_3OH and $HCOOCH_3$ on ZnO and TiO_2 are shown in Figs. 5 - 8, respectively.

Infrared study of surface species

The IR spectra of surface species formed on ZrO_2, ZnO and TiO_2 during a CO adsorption cycle (25 → 500 → 25 °C) are compared in Figs. 9a, 9b and 9c, respectively. The spectrum on ZrO_2, Fig. 9a, is from ref. 6. The spectra of Fig. 9b and c were taken after heating the ZnO and TiO_2 wafers in CO (200 torr) to 500 °C within the IR cell, cooling to 25 °C and evacuating at 10^{-3} torr. The absorption bands detected in Fig. 9b were 2955 (trace), 2880, 1580, 1410 and 1365 cm^{-1}, while those detected in Fig. 9c were 2955, 2875, 1560 and 1360 cm^{-1}.

The interconversion between surface methoxide and surface formate was checked by IR. In Fig. 10, methanol (20 torr) was adsorbed on the surface of ZnO after heating the sample in vacuum to 500 °C, cooling to 25 °C and dosing with methanol. The spectrum, Fig. 10a, was recorded after evacuation at 25 °C for 0.25 h. There are two relatively strong absorption bands, at 2935 and 2820 cm^{-1}, and some weaker signals in the region 1300 -

TABLE 3

TPD/TPDE of CH_3OH, HCOOH and $HCOOCH_3$ adsorbed on ZrO_2, ZnO and TiO_2 (into flowing H_2 except where noted)

Oxide	Gas adsorbed	Product desorption temperature peak regions			
		100 - 250 °C[a]	250 - 400 °C	400 - 500 °C	500 - 650 °C
ZrO_2	CH_3OH	CH_3OH, H_2CO, CH_4, CO		CH_4, CO	CH_3OH, CO_2, CO
	HCOOH	CO	CO, CO_2, H_2CO, HCOOH	CH_4	CH_3OH, CO_2, CO
	HCOOH (in He)	CH_4	CO, CO_2, H_2CO, H_2		CO_2, CO, CH_4, H_2
	$HCOOCH_3$	CH_3OH, H_2CO, CH_4, CO		CH_4, CO, CO_2	CH_3OH, CO_2, CO
ZnO	CH_3OH	CH_3OH, H_2CO, CH_4, CO	CO, CO_2	CH_4	CH_3OH, H_2CO, CH_4
	HCOOH			CO, CO_2, H_2CO, CH_3OH, CH_4, HCOOH	
	HCOOH (in He)		H_2, CO, CO_2, CH_4, H_2CO	H_2, CO_2, CO	
	$HCOOCH_3$	H_2CO, CH_3OH, CH_4, CO, CO_2	CO	CH_4	H_2CO, CH_3OH
TiO_2	CH_3OH	CO, H_2CO, CH_3OH, CH_4	CO	CH_4, CO	
	HCOOH		CO	CH_4, CO, CO_2	
	HCOOH (in He)		CO	CO	
	$HCOOCH_3$	$HCOOCH_3$	H_2CO, CH_3OH, CO, CH_4, CO_2	CH_4, CO, CO_2	

[a]These temperature regions defined for qualitative comparison only.

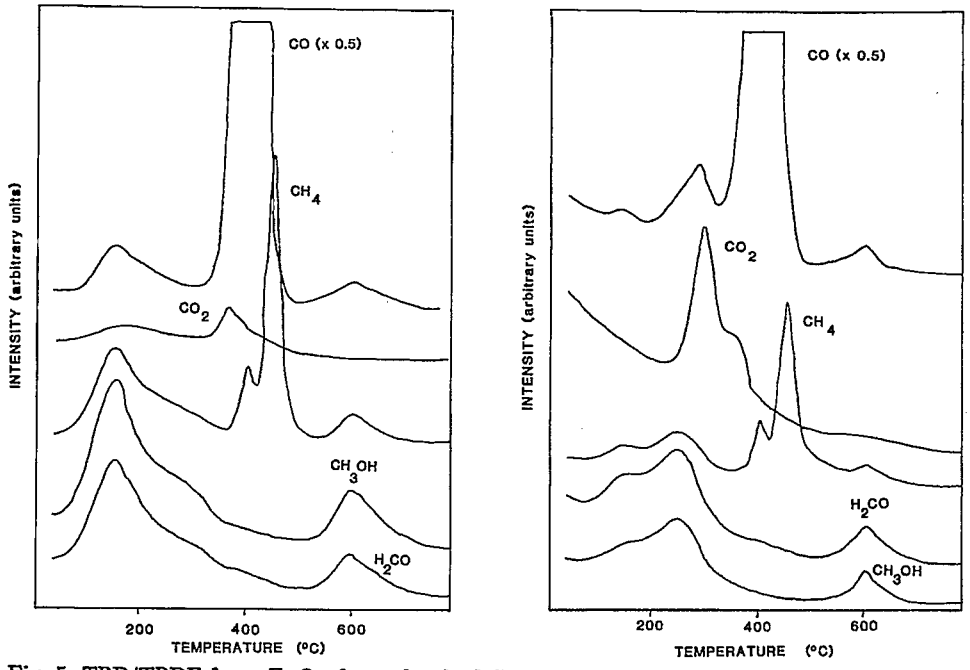

Fig. 5. TPD/TPDE from ZnO of preadsorbed CH_3OH into flowing H_2.
Fig. 6. TPD/TPDE from ZnO of preadsorbed $HCOOCH_3$ into flowing H_2.

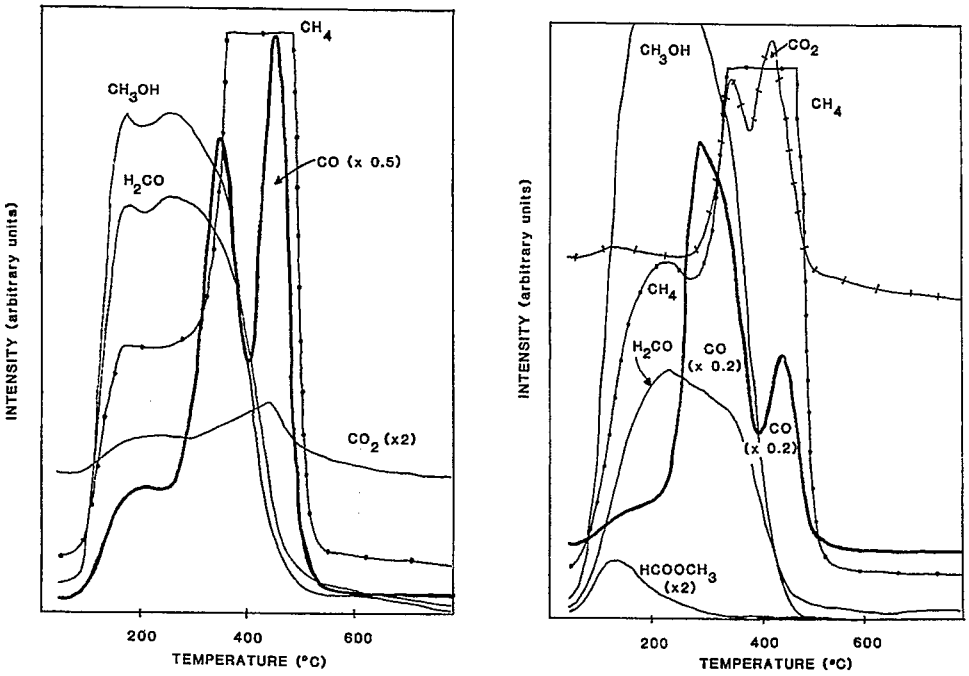

Fig. 7. TPD/TPDE from TiO_2 of preadsorbed CH_3OH into flowing H_2.
Fig. 8. TPD/TPDE from TiO_2 of preadsorbed $HCOOCH_3$ into flowing H_2.

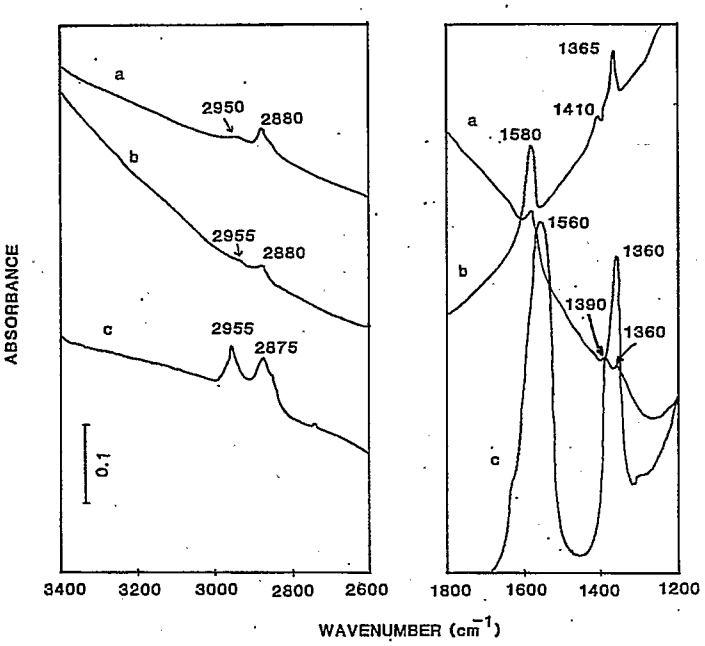

Fig. 9. IR spectra of species formed during a CO adsorption cycle on (a) ZrO_2, (b) ZnO and (c) TiO_2.

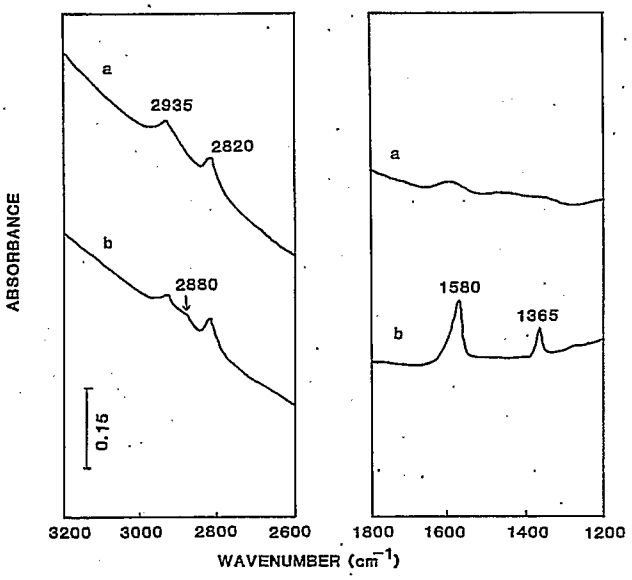

Fig. 10. IR spectra of species formed by adsorption of CH_3OH on ZnO. Spectra were taken after dosing at 25 °C and (a) evacuation at 25 °C for 0.25 h, (b) evacuation at 200 °C for 0.25 h.

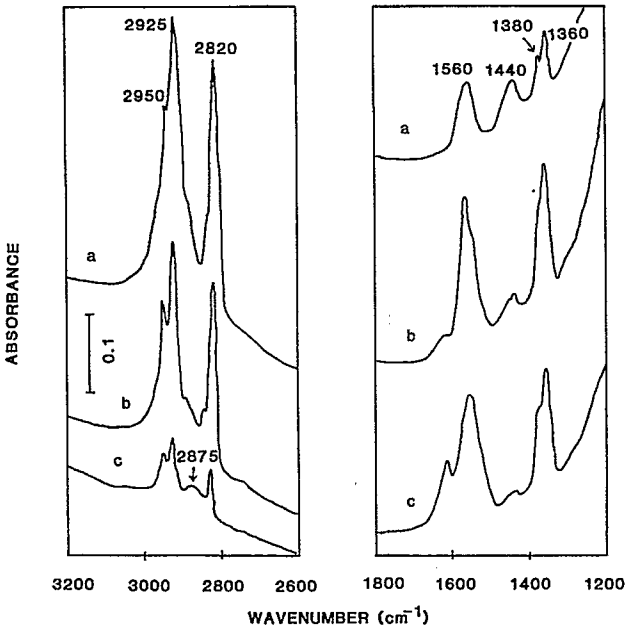

Fig. 11. IR spectra of species formed by adsorption of CH_3OH on TiO_2. Spectra were taken after dosing at 25 °C and (a) evacuation at 25 °C for 0.25 h, (b) heating in oxygen at 200 °C for 0.25 h, and (c) heating in oxygen at 300 °C for 0.25 h.

1600 cm^{-1}. Figure 10b was obtained after this sample was heated in vacuum at 200 °C for 0.25 h. Strong bands at 1580 and 1365 cm^{-1} and a smaller band at 2880 cm^{-1} appeared during this treatment.

The results of methanol adsorption on TiO_2 are shown in Fig. 11. Figure 11a was recorded after methanol (20 torr) adsorption on TiO (25 °C) and evacuation (25 °C, 0.25 h). Figures 11b and 11c were recorded after oxygen treatment at 200 °C (0.25 h) and 300 °C (0.25 h) respectively. The major bands of Fig. 11a are at 2950, 2925, 2820, 1560, 1440, 1380 and 1360 cm^{-1}. All these bands also appear in Figs. 11b and 11c. However, the intensity in the region 2800 - 3000 cm^{-1} was attenuated strongly while the intensity in the region 1300 - 1600 cm^{-1} increased. A new band, at 2875 cm^{-1}, is distinguishable in Fig. 11c.

Methanol formation on ZnO at low temperature

Methanol synthesis from $CO/H_2/H_2O$ on ZrO_2 at low temperature (150 - 200 °C) is reported elsewhere [8]. The same experiments with ZnO and TiO_2 do not produce methanol at any temperature. In the absence of water, methanol is produced on ZnO while heating an oxygen-treated sample in CO/H_2 in the temperature range 200 - 300 °C. Even in the absence of H_2O, no methanol was ever observed in TPD/TPDE from TiO_2.

Discussion

As noted earlier, a detailed discussion has been given of the species formed on ZrO_2 and their decomposition behavior [5, 6]. The assignments made here for ZnO and TiO_2 are based on analogies with that data and literature on these oxides. Our goal is to develop a mechanistic scheme which correlates all the data in a single representation and which shows the common reaction paths as well as the differences. This summary is given in Fig. 12. In the discussion which follows, we present the available evidence for these paths.

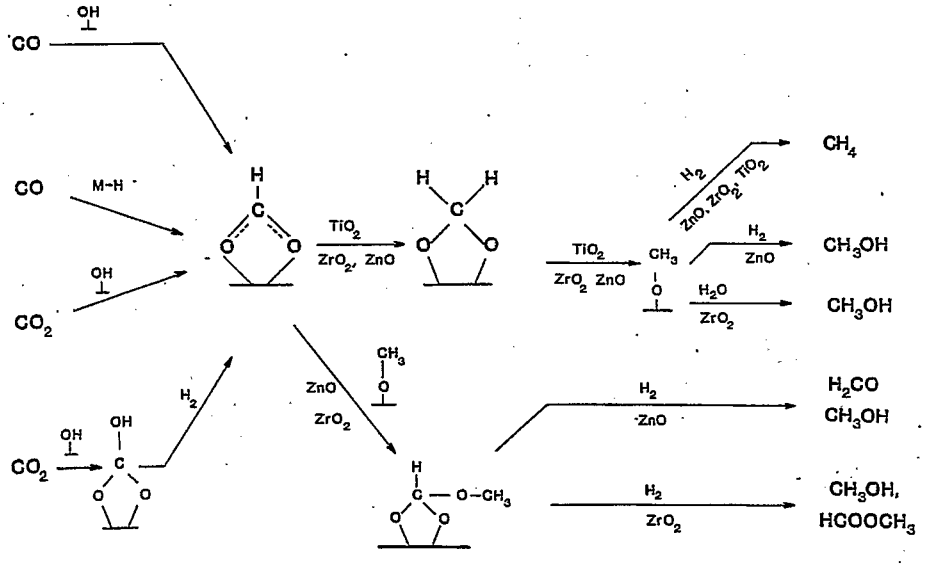

Fig. 12. Mechanistic scheme for reactions of CO/H_2 and CO_2/H_2 mixtures over ZrO_2, ZnO and TiO_2.

Referring to Table 2, the lowest temperature desorption region (I) is assigned to adsorbed molecular CO on the basis that it is the only product detected in this regime, that this desorption peak appears only after the sample is exposed to CO, and that IR spectra show the loss of CO stretching modes upon evacuation in this temperature region [31]. Further discussion of this region is unnecessary.

Desorption in regions (II) and (III) is assigned to surface carbonate species with no further delineation into bidentate, monodentate or bicarbonate species. As shown in Table 2, desorption in this region leads only to CO and CO_2, with CO_2 generally dominant. Carbonate speciates have been observed by IR upon adsorption of CO and/or CO_2 [6, 10, 29, 30, 32, 35]. The carbonates may arise as the result of a bicarbonate intermediate as follows (for TiO_2):

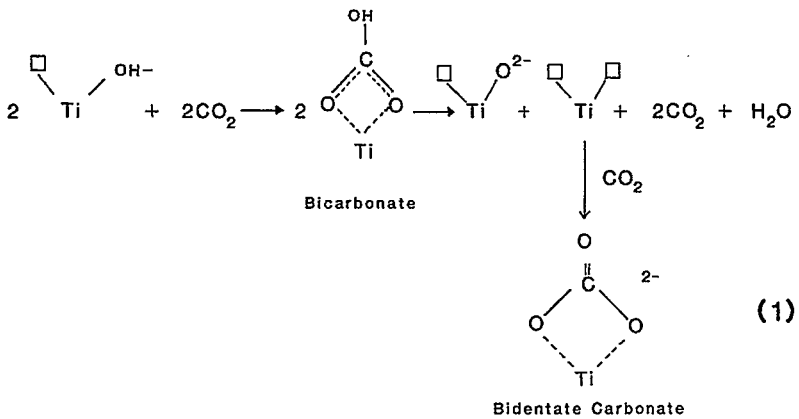

(1)

In Fig. 9b a small band at 1410 cm^{-1} appears after exposure of ZnO to CO over the temperature range 25 to 500 °C. We take this to be consistent with the formation of bicarbonates [29, 30]. Other carbonate bands in this region are not resolved, perhaps because the system is dominated by formate.

In previous work, formate bands at 2870, 1571 and 1367 cm^{-1} appeared upon adsorption of CH_3OH on ZnO [36]. Similar bands (Fig. 9b) appear after exposure of ZnO to CO at 500 °C, establishing that formate formation from CO occurred. The TPD/TPDE spectrum in Table 3 of adsorbed formate (derived from formic acid) in flowing He gives, in region III, $CO_2 > H_2 > CO$, indicating that ZnO works as a dehydrogenation catalyst in this circumstance. The products formed in region II result from the desorption/decomposition of surface species in the presence of molecular HCOOH. The desorbed species differ from those formed when desorbing into H_2. For example, in Table 3 the formation of CH_4 from formic acid clearly requires the addition of hydrogen to the system.

In the case of TiO_2, surface formate has been observed upon adsorption of either formic acid [38] or formaldehyde [32]. The formate bands were at 2890, 1590, 1385 and 1365 cm^{-1} [32]. These are about 25 cm^{-1} higher than observed here after CO exposure to TiO_2 at 500 °C (Fig. 9c shows bands at 2875, 1560 and 1360 cm^{-1}). We attribute these changes to differences in the surface structures of the titanias used (*e.g.*, anatase-to-rutile ratio and degree of reduction of the surface).

Surface carbonate on TiO_2 have been reported in IR studies with bands in the 1330 - 1420 and 1570 - 1600 cm^{-1} regions [29, 30, 39]. Although no distinct carbonate bands are found in Fig. 9c, they may lie within and beneath the bands assigned here to formate. According to Table 3, desorption into He of species derived from formic acid gives CO, not CO_2 and H_2. Evidently surface formates are dehydrated, rather than dehydrogenated, on TiO_2. The water of dehydration appears as a broad and weak signal.

Adsorption of methanol on a broad range of metal and metal oxides leads to methoxide [26, 36, 40 - 44]. The IR spectra are characterized by a C—H symmetric stretch near 2840 - 2820 cm^{-1}. On ZnO and TiO_2 we find

bands in this region (Figs. 10 and 11) which are also attributed to methoxide. Oxidation of this methoxide species to formate occurs upon heating either in vacuum or in oxygen (Figs. 10b, 11b and 11c). A similar interconversion has already been established for ZrO_2 [6]. In passing, we note that the bands in the 2955 - 2965 cm^{-1} region of Figs. 9b and 9c can be assigned to surface methoxide and/or oxymethylene (H_2COO^-) [8].

The TPD/TPDE into H_2 of surface methoxide from methanol adsorption leads to CH_4, as indicated in Table 3. Similar production of CH_4 is found after adsorption of formic acid and methyl formate (Table 3 and Figs. 5 - 8), indicating that surface methoxide may be a common intermediate. Further, for each of the three oxides the TPD/TPDE into H_2 after exposure to CO leads to CH_4 in similar temperature regimes, suggesting that methoxide is a common intermediate in the reaction path leading to methane.

When TPD/TPDE of adsorbed HCOOH was done into He, however, the product distributions and temperature distributions shifted towards those characteristic of formate, *i.e.*, CO_2 and H_2 or CO and H_2O, with very little methane. This result indicates that surface formate is a precursor to methoxide in the hydrogenation sequence.

On ZnO there is a low-temperature methanol peak (Table 3) in the TPD/TPDE of methyl formate. A similar CH_3OH peak is observed when ZnO is heated in CO/H_2 to 600 °C, cooled to room temperature and reheated in CO/H_2. As for ZrO_2 [8], the immediate precursor to this methanol is thought to be methoxide, with formate participating at an earlier stage. However, ZrO_2 and ZnO differ in that adsorbed H_2O is required for ZrO_2, but its absence is required on ZnO. This difference may be related to the ability of ZnO to form significant amounts of Zn—H during exposure to H_2, whereas on ZrO_2, Zr—OH is important. Schematically these paths are illustrated as follows:

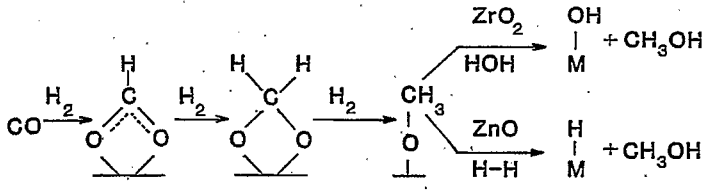

In this model, H_2O could inhibit CH_3OH formation on ZnO by blocking sites for Zn—H formation.

High-temperature methanol forms on ZrO_2 and ZnO but not on TiO_2 (Tables 2 and 3). Methyl formate is observed in the products during methanol production from synthesis gas [2, 45]. Methyl formate was observed when pre-adsorbed $HCOOCH_3$ on ZrO_2 was desorbed into He [8] and when CO/H_2- or CO_2/H_2-treated ZrO_2 was heated in H_2 (Table 2). The high-temperature data in Table 3 following $HCOOCH_3$ adsorption and the appearance of methanol at high temperature over ZnO and ZrO_2 (Table 2) suggest a common precursor. It is proposed that this methanol derives from a surface methyl formate-like intermediate. This intermediate was postulated to form

by nucleophilic attack of CH_3O^- [8, 46] on formyl [46] or formate [8]. The structure of the methyl formate-like species depends on the reactants from which it is formed as follows:

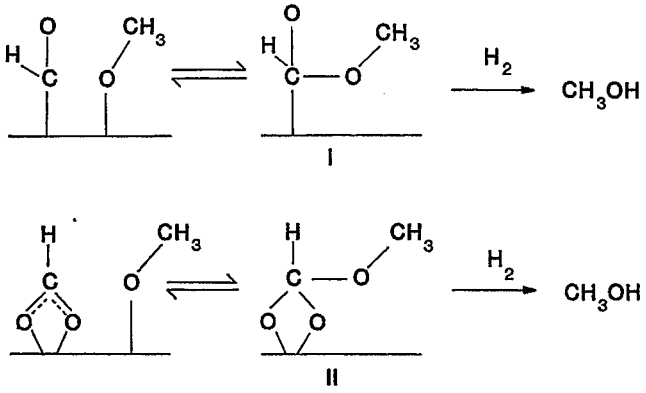

Structures I and II have been proposed previously [8, 46]. We favor structure II over ZnO because it is formed from formate which we know to be present in our experiments. The formation of methanol from formaldehyde through a methyl formate intermediate has been proposed on a number of metal oxides [47]. Both acidic and basic sites are implicated [47 - 49]. This is consistent with the present results in that TiO_2 is very acidic, while ZrO_2 and ZnO have both acid and base sites.

On all three oxides studied here, surface OH groups are significant. On ZrO_2, evidence is provided by D—H labeling studies [5, 6]. On ZnO and TiO_2, surface formates are detected after CO adsorption in the absence of H_2. In the presence of H_2, reaction between CO and surface Zn—H must also be considered for ZnO.

We propose that on all three metal oxides, the surface formate is the key intermediate in the hydrogenation of either CO or CO_2. Other intermediates, for example methoxide and the methyl formate-like species, are derived from it and lead to the desorbing hydrogenated products — CH_4, H_2CO and CH_3OH. The scheme in Fig. 12 is consistent with the experimental observations and involves this common formate intermediate and different subsequent reaction paths.

Conclusions

Using IR and TPD/TPDE techniques to study CO/H_2 and CO_2/H_2 hydrogenation and related systems (CH_3OH, HCOOH and $HCOOCH_3$) on ZrO_2, ZnO and TiO_2 catalysts, a reaction path scheme has been developed which involves a common formate intermediate. This intermediate is followed by various amounts of methoxide and methyl formate in leading to the observed hydrogenation products.

On ZrO_2 and ZnO, methanol can be formed and desorbed either at low (100 - 300 °C) or high (580 - 610 °C) temperature. On TiO_2, methanol is not observed. On ZrO_2, the low temperature methanol formation requires H_2O; while for ZnO, H_2O must be absent.

Acknowledgements

M.-Y. H. thanks the Research Institute of Petroleum Processing (Beijing, P.R.C.) for a leave of absence. This work was supported in part by the Division of Chemical Sciences, Office of Basic Energy Sciences, U.S. Department of Energy under Contract DE-AS05-80ER1072 (J.G.E.), the Office of Naval Research (J.M.W.) and the University of Texas Center for Energy Studies.

References

1 C. K. Rofer-DePoorter, *Chem. Rev., 81* (1981) 447.
2 K. Klier, *Adv. Catal., 31* (1982) 243.
3 H. H. Kung, *Catal. Rev., 22* (1980) 235.
4 B. Denise and R. P. A. Sneeden, *J. Mol. Catal., 17* (1982) 359.
5 M.-Y. He and J. G. Ekerdt, *J. Catal., 87* (1984) 238.
6 M.-Y. He and J. G. Ekerdt, *J. Catal., 87* (1984) 381.
7 M.-Y. He and J. G. Ekerdt, *CO and CO_2 Hydrogenation over Zirconium Dioxide*, Div. Petrol. Chem., Am. Chem. Soc. St. Louis Meeting, April 8 - 13, 1984.
8 M.-Y. He and J. G. Ekerdt, *J. Catal., 90* (1984) 17.
9 F. Boccuzzi, E. Garrone, A. Zecchina and A. Bossi, *J. Catal., 51* (1978) 160.
10 J. Saussey, J.-C. Lavalley, J. Lamotte and T. Rais, *J. Chem. Soc., Chem. Commun.*, (1982) 278.
11 J.-C. Lavalley, J. Saussey and T. Rais, *J. Mol. Catal., 17* (1982) 289.
12 G. Henrici-Olivé and S. J. Olivé, *J. Mol. Catal., 17* (1982) 89.
13 M. Bowker, H. Houghton and K. C. Waugh, *J. Chem. Soc., Faraday Trans. 1, 77* (1981) 3023.
14 M. Bowker, H. Houghton and K. C. Waugh, *J. Chem. Soc., Faraday Trans. 1, 78* (1982) 2573.
15 M. Bowker, H. Houghton, K. C. Waugh, T. Giddings and M. Green, *J. Catal. 84* (1983) 252.
16 R. P. Eischens, W. A. Pliskin and M. J. D. Low, *J. Catal., 1* (1962) 180.
17 F. Boccuzzi, E. Borello, A. Zecchina, A. Bossi and M. Camia, *J. Catal., 51* (1978) 150.
18 R. Eisenberg and D. E. Hendricken, *Adv. Catal., 28* (1979) 79.
19 R. Ugo and R. Psaro, *J. Mol. Catal., 20* (1983) 53.
20 G. Henrici-Olivé and S. Olivé, *Angew. Chem., Int. Ed. Engl., 15* (1976) 136.
21 C. P. Casey, S. M. Neumann, M. A. Andrews and D. R. McAlister, *Pure Appl. Chem., 52* (1980) 625.
22 T. van Herwijnen and W. A. deJong, *J. Catal., 63* (1980) 83.
23 A. Ueno, T. Onishi and K. Tamaru, *Trans. Faraday Soc., 66* (1970) 756.
24 A. Deluzarche, R. Kieffer and A. Muth, *Tetrahedron Lett., 38* (1977) 3357.
25 I. E. Wachs and R. J. Madix, *J. Catal., 53* (1978) 208.
26 M. Bowker and R. J. Madix, *Surf. Sci., 95* (1980) 190.
27 R. J. Madix, *Adv. Catal., 29* (1980) 1.

28 A. Takenchi and J. R. Katzer, *J. Phys. Chem., 85* (1981) 937.
29 K. Tanaka and J. M. White, *J. Phys. Chem., 86* (1982) 24.
30 K. Tanaka and J. M. White, *J. Phys. Chem., 86* (1982) 3977.
31 K. Tanaka and J. M. White, *J. Catal., 79* (1983) 81.
32 R. P. Groff and W. H. Manogue, *J. Catal., 79* (1983) 462.
33 E. E. Ibok and D. F. Allix, *J. Catal., 66* (1980) 391.
34 R. J. Gorte, *J. Catal., 75* (1982) 164.
35 L. H. Little, *Infrared Spectra of Adsorbed Species,* Academic Press, New York, 1966.
36 A. Vens, T. Onishi and K. Tamaru, *Trans. Faraday Soc., 67* (1971) 3585.
37 J. H. Taylor and C. H. Amberg, *Can. J. Chem., 39* (1961) 535.
38 G. Munuera, *J. Catal., 18* (1970) 19.
39 C. E. O'Neill and D. J. C. Yates, *Spectrochim. Acta, 17* (1961) 953.
40 G. Blyholder and W. V. Wyatt, *J. Phys. Chem., 70* (1966) 1745.
41 R. O. Kagel and R. G. Greenler, *J. Chem. Phys., 49* (1968) 1638.
42 Y. Soma, T. Onishi and K. Tamaru, *Trans. Faraday Soc., 65* (1969) 2215.
43 R. G. Greenler, *J. Chem. Phys., 37* (1962) 2094.
44 W. Hertle and A. M. Guenca, *J. Phys. Chem., 77* (1969) 1120.
45 K. Frolich Per, M. R. Fenski and D. Quiggle, *Ind. Eng. Chem., 20* (1928) 694.
46 E. L. Muetterties and J. Stein, *J. Chem. Rev., 79* (1979) 479.
47 M. Ai, *J. Catal., 83* (1983) 141.
48 M. Ai, *J. Catal., 77* (1982) 279.
49 K. Tanaka and K. Saito, *J. Catal., 35* (1974) 247.